Sputtering of Ordered Ice I_h Adsorbed on Rh(111) Using Hyperthermal Neutral Ar Atoms

K. D. Gibson, D. R. Killelea, and S. J. Sibener*

The James Franck Institute and Department of Chemistry, The University of Chicago, 929 East 57th Street, Chicago, Illinois 60637

Received: February 28, 2009; Revised Manuscript Received: May 16, 2009

The sputtering of ordered overlayers of water physisorbed on Rh(111) by hyperthermal Ar atoms was investigated. For incident kinetic energies of 10 to 20 eV, the impact of the Ar atoms leads to the desorption of intact single water molecules. This sputtering is sensitive to the crystalline structure of the ice overlayers with the intensity and energy of the sputtered molecules being dependent upon both the final polar and azimuthal angles. The similarity between the results for one and three layers of water strongly suggests that all of the sputtering originates from the exposed topmost layer. In all cases sputtering yields are small, $\sim 10^{-3}$, and decreases with increasing film thickness; most of the energy transferred during the collision is dissipated into the lattice. These results suggest that sputtering of surfaces with hyperthermal neutrals might be useful as a noncharging and nonchemically destructive adjunct to ion-induced sputtering and secondary ion mass spectroscopy for compositional depth profiling and trace analysis. Intact neutral molecules are ejected, and the molecules left on the surface have not been altered, which is not the case for ion sputtering.

Introduction

The sputtering of materials by collisions with high-energy particles has been extensively studied due to its key role in such technologically important processes as ion-implantation, chemically sensitive surface analysis such as secondary ion mass spectroscopy (SIMS), and the sputtering of adsorbed gases from the walls of fusion reactors, which is a source of significant energy losses in the plasma.[1,2] Much of the work involves the use of ion beams, which are relatively easy to produce and focus.[3,4] In general, the ion kinetic energies used vary from a few hundred to many thousand electron volts.

One use for low-energy ion sputtering is depth profiling of thin organic films,[5] where the chemical composition of the exposed surface of the film is examined by a technique such as X-ray photoelectron spectroscopy while layers of material are progressively removed. A major problem with using ions to remove material is that the surface is often chemically altered.[6] This motivated us to investigate whether using hyperthermal neutrals could avoid this problem, but still effectively remove material on a layer-by-layer basis.

There have been several studies where neutral atoms were used for sputtering (incident energies of a few to tens of electron volts), including collision-induced desorption[7−9] and the sputtering of ions from semiconductor surfaces.[10] The first two studies[7,8] are the most relevant to our experiments. Both used Ar beams to collisionally desorb a monolayer of weakly physisorbed adsorbates, CH_4[7] or Xe.[8] In both cases, the yield (Y = atoms or molecules desorbed/incident Ar) approached unity for incident Ar kinetic energies well below 10 eV. The mechanisms involved might well be different for a monolayer on a metal surface, rather than a thicker layer of a "soft" material, but these results suggest that the technique might have some value for depth profiling measurements.

We wish to expand on our knowledge of sputtering with neutral atoms, particularly for films thicker than one layer. For our model, we used ordered overlayers of ice adsorbed on a Rh(111) surface. Though not an organic system, the molecule−molecule binding energy, in this case dominated by hydrogen bonds, is relatively low. In addition, the overlayer is nonconducting, so that incoming ions are not neutralized before contact with the surface, allowing for a direct comparison of the interaction of neutrals versus ions. We also had previous experience growing ordered thin film ice structures,[11] and some previous ion sputtering papers for comparison purposes.

The ion sputtering experiments that come closest to the conditions described in our paper are those of Fama et al.[12] in which an amorphous ice surface was bombarded with 350 eV Ar^+ ions. At this energy, the yield is approximately three. Even closer to the conditions of the present paper is the theoretical study of Brenner and Garrison,[13] where O^+ ion bombardment of a {110} ice surface with incident energies as low as 23 eV and normal incidence angle was simulated. For the lowest collision energy, the yield was 0.83 with the sputtered H_2O coming off intact, mainly as single molecules, but a few small clusters were predicted. The kinetic energy of the escaping H_2O molecules was calculated to be principally below 1 eV; 97% came from the top layer and the rest from the second layer.

To summarize, we will discuss the sputtering of water molecules from ordered thin films of ice, one to eight layers thick, grown on a Rh(111) surface. The incident particles were neutral Ar atoms with kinetic energies between 10 and 20 eV. This allows us to compare the relative efficiency for sputtering using either charged or uncharged particles.

Experimental Details

The scattering experiments were carried out in an ultra-high vacuum (UHV) chamber with a base pressure of 1×10^{-10} Torr.[14,15] The Rh(111) sample was mounted on a rotating manipulator so that the incident polar (Θ) and azimuthal angles could be varied. The crystal can be resistively heated and cryogenically cooled with liquid N_2. There is a separately rotating, double-differentially pumped quadrupole mass spec-

* To whom correspondence should be addressed. E-mail: s-sibener@uchicago.edu.

10.1021/jp901874d CCC: $40.75
Published on Web 07/01/2009

trometer (electron-bombardment ionization, ~1 degree fwhm angular resolution) to detect the scattered Ar and sputtered H_2O.

The hyperthermal translational energy Ar atoms were produced with a source originally developed by Physical Sciences, Inc.[16] and further refined by the Minton group.[17] A pulse of Ar is produced from a piezoelectric pulsed valve inspired by the Proch and Trickl design.[18] The Ar expands into a gold-plated Cu cone. After a delay of 200−300 μs, a pulsed CO_2 laser is fired and the light is focused into the narrow end of the cone with a spherical mirror (1 m radius of curvature), where it induces a breakdown and rapidly heats the gas to more than 20 000 K. The hot gas expands from a confined region of space, making the source effectively a point source. However, the gas pulse that exits the conical nozzle has a fairly broad velocity distribution. Therefore, a single synchronized chopper wheel 21.21 cm from the crystal position is used to select a portion of the initial velocity profile. The chopper wheel also blocks all of the light emitted by the source plasma and essentially all the residual ions, which travel at significantly greater velocities than most of the atoms in the neutral beam pulse. After the Ar collides with the surface, we measure either the scattered Ar or sputtered H_2O distributions by time-of-flight (TOF) spectroscopy, using a multichannel scaler system. The crystal to ionizer flight path measures 14.45 cm. The crystal can be lowered out of the beam path and the detector positioned directly in the path of the hyperthermal Ar beam. This allows the direct measurement of the velocity distributions of the incident beam. The lowest incident energy used had an average of 10.4 eV with a full width at half maximum (FWHM) of 5 eV, and the highest energy was 21 eV with a FWHM of 11 eV. An example TOF spectrum of sputtered H_2O and the energy distribution derived from fitting the data are shown in Figure 1. The fitting procedure is a nonlinear least-squares routine, using a forward convolution of a flux-weighted velocity distribution with the instrument function. The fitting procedure adjusts the velocity distribution parameters to give the best least-squares fit to the experimental data. This derived velocity distribution can then be used to derive the energy distribution and average quantities such as the intensities and energies.

The Rh crystal was cut within 1° of the (111) face as determined by Laue X-ray backscattering. Cleaning involved cycles of Ar^+ ion sputtering and O_2 exposure at 900 K, followed by annealing at 1200−1300 K. Cleanliness was confirmed by Auger electron spectroscopy and He atom reflectivity. He atom diffraction was also used to align the azimuthal direction with the scattering plane determined by the incident beam and detector.

The growth of ordered H_2O overlayers on Rh(111) was extensively covered in a previous paper.[11] It forms a $(\sqrt{3} \times \sqrt{3})$R30° overlayer structure. The O atoms on the hexagonal face are probably slightly buckled,[19] so that a single layer of H_2O is called a bilayer. In the present paper, the coverage will be referred to as multiples of this bilayer, so that the thinnest coverage, a single bilayer, will be referred to as one layer, and further thicknesses will be given as multiples of this coverage. The overlayers are grown by exposing the Rh to molecular beams of H_2O or D_2O entrained in He, produced by bubbling the carrier gas through room temperature reservoirs of the liquid, resulting in a flux at the surface of ~0.2 layers/sec. The procedure was the same as reported previously.[11] In brief, the clean Rh(111) substrate was exposed to an O_2 beam at T_s = 350 K so as to adsorb ~0.05 monolayers of dissociated O. The sample is cooled and exposed to the H_2O or D_2O beams. The initial surface temperature for dosing ($T_S \simeq 160$ K) is controlled

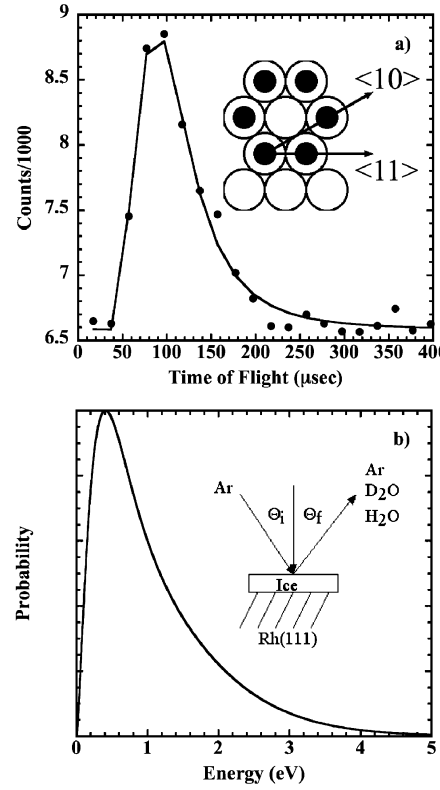

Figure 1. (a) TOF spectrum of sputtered H_2O from a three layer film. Points are the data, and the solid line is the fit. Conditions are Θ_i = 45°, Θ_f = 55°, <10> azimuth, T_s = 125 K, and an average translational energy of 10.4 eV for the Ar. The inset shows a schematic of a single layer of water (filled circles are O of the H_2O) adsorbed on Rh(111) (large open circles). Arrows show the azimuthal directions. (b) The derived flux-weighted energy distribution and the inset explains the scattering geometry.

so that only a single layer, but not multiple layers, can be grown. This procedure gives a well-ordered single layer as determined by He diffraction. Further overlayers are grown by exposure at a slightly lower surface temperature ($T_S \simeq 145$ K), close to the multilayer desorption temperature. Multilayer coverage is determined by temperature-programmed desorption (TPD), and comparing the integrated signal to that of a single layer. Example TPD spectra are shown in the previous paper.[11]

Results and Discussion

Figure 2 shows a series of sputtered H_2O TOF spectra for an incident Ar energy of 21 eV and Θ_i = 45°. Figures 3−7 show the derived results with the average energy of the sputtered molecules in the top panel and the integrated intensity in the bottom panel. Each spectrum in Figure 2 corresponds to one square point in Figure 3. For all of the data shown, the intensity has been normalized by the incident Ar flux and corrected for the instrument geometry, so that the intensities can be directly compared between any of the figures. Representative error bars are plotted for points where there were three or more spectra taken at the same conditions.

We only observed individual water molecules during hyperthermal Ar exposure. To check for the ejection of clusters, the mass spectrometer was tuned to m/e = 36 amu, but no $(H_2O)_2$ was detected. Since the detector has a large m/e = 19 background signal, we did not look for H_3O^+, which should be a major fragment from $(H_2O)_2$ ionization. The absolute yield, Y = sputtered H_2O molecules per incident Ar atoms, was roughly estimated by comparing the m/e = 40 signal for the Ar

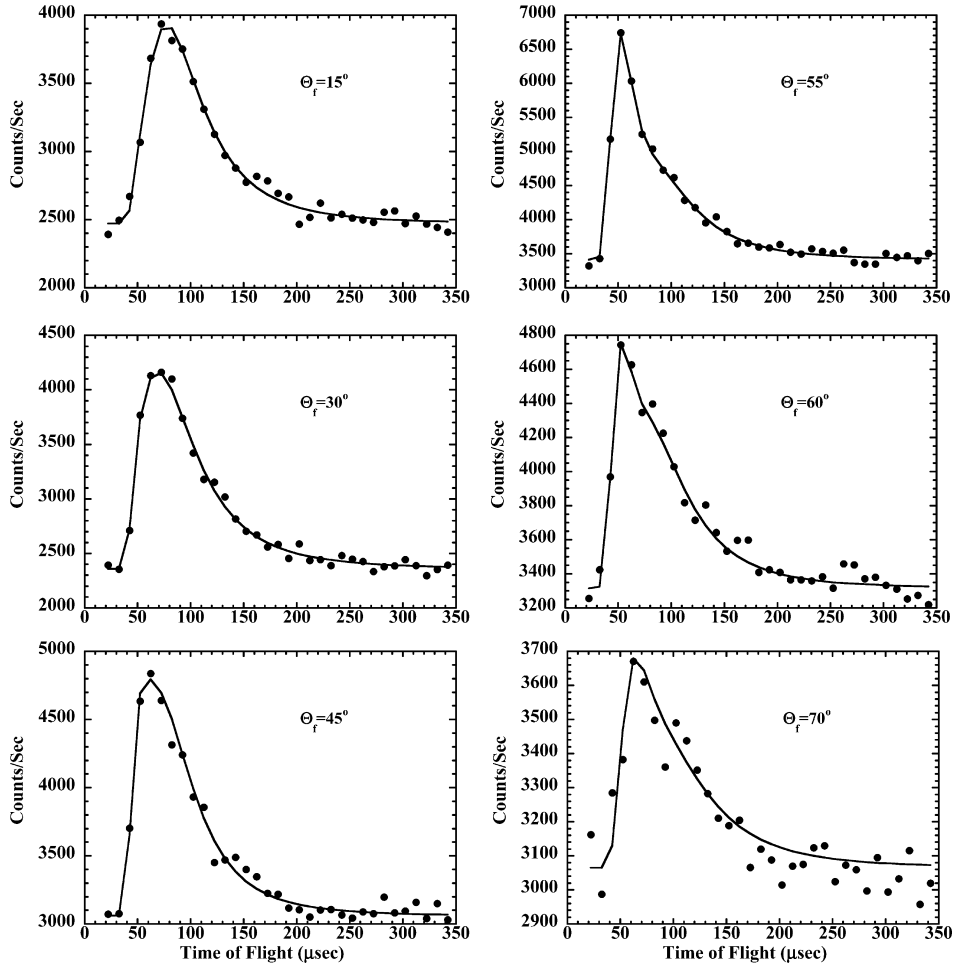

Figure 2. Sputtered H_2O TOF spectra for a three layer film with $T_s = 125$ K, $\Theta_i = 45°$, and an incident Ar energy of 21 eV. Points are the data and the line is the fit.

beam to the $m/e = 18$ signal for the water beam, both measured with the detector directly in the beam path. The water beam flux was determined by the amount of ice build-up from exposing the 125 K Rh(111) surface. At this surface temperature, the sticking coefficient was assumed to be 1, because no scattered water was observed in the scattering chamber with the residual gas analyzer or the detector. The result is a flux per pulse of ca. 10^{13} Ar atoms/cm^2. This, combined with the amount of water molecules sputtered (at most ~0.05 of a layer), measured by postexposure TPD, gives an order of magnitude estimate for Y of 10^{-3}. These values are much lower than expected from an extrapolation of the observed yield for Ar^+ ions[12] and orders of magnitude lower than calculated for 23 eV O^+.[13]

Figures 3−5 show the sputtering of three layers of H_2O, along the two principal azimuths, for incident angles, Θ_i, of 20 and 45°, and average energies for the incident Ar of between 10 and 20 eV. It is apparent that there is a distinct difference between the angular energy and intensity distributions for the two azimuths. In the <11> direction, there is a distinct maximum for both incident angles at the final angle, Θ_f, of ~55°. This is independent of the Ar incident angle and initial kinetic energy. The sputtered water molecules carry no more than ~10% of the incident Ar energy.

Figure 6 compares the results for one and three layers of H_2O. The angular energy distributions of the sputtered water are identical within our experimental error. The rate of H_2O sputtering appears slightly higher from one layer as compared to three layers, but the yield is still much lower than those observed for physisorbed CH_4[7] or Xe.[8] The single layer is in direct contact with the Rh(111) surface as compared with the two water layers under the surface of the three layer film. That the scattering is so similar strongly suggests that the sputtering is principally due to Ar collisions with and interactions between only molecules on the surface. Even if the sputtered water is produced by a secondary collision with a water molecule displaced by the original Ar-surface collision, the mechanism still only involves surface molecules. This is in qualitative agreement with what is known for low-energy ion sputtering.[2,4,13]

Figure 7 shows the results for the Ar sputtering of eight layers of D_2O adsorbed on Rh(111). As was observed for the growth of water on Ru(001), thicker layers sputtered more slowly.[20,21] The low sputtering rate combined with a relatively high mass 18 background in the detector prompted the use of the deuterated isotopologue of water, since the mass 20 background was quite low. This leads to improved statistics due to greater signal-to-noise ratio. The use of D_2O did require that the Ar scattering from the surface also be measured to correct for the signal at $m/e = 20$ due to Ar^{2+}. Comparing the results for the two symmetry directions, there may be a shape similar to that of the angular intensity distributions of the thinner layers, but we are hesitant to infer too much from this as the data are close to the limits of experimental error. Not shown are some measurements from a 50 layer film where the sputtered D_2O signal is further reduced to ~20% of sputtered signal from 8 layers.

Figure 8 shows the average energy and intensity of the scattered Ar as a function of the scattering angle. As with the scattering from other soft materials, for example Ar from a decanethiol overlayer,[22] the TOF spectra could be fit with two

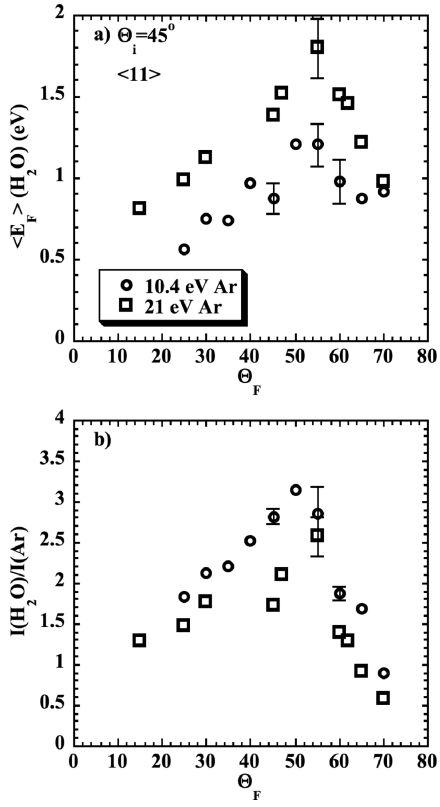

Figure 3. The average energy and integrated intensity for water molecules sputtered from three layers of H_2O as a function of Θ_f for two different Ar translational energies are plotted. Conditions are $\Theta_i = 45°$, <11> azimuth, and $T_s = 125$ K.

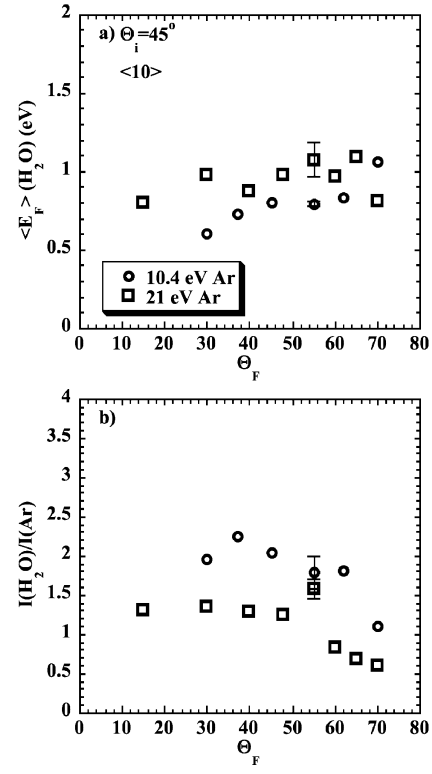

Figure 4. The average energy and integrated intensity for water molecules sputtered from three layers of H_2O as a function of Θ_f for two different Ar translational energies are plotted. Conditions are $\Theta_i = 45°$, <10> azimuth, and $T_s = 125$ K.

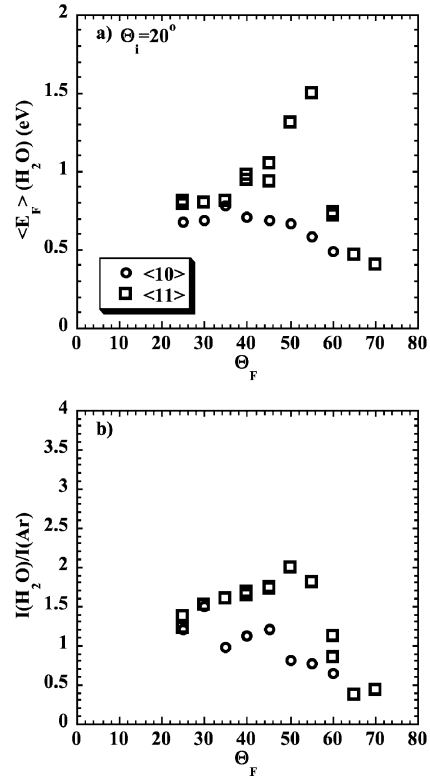

Figure 5. The average energy and integrated intensity for water molecules sputtered from three layers of H_2O as a function of Θ_f are plotted. Conditions are $\Theta_i = 20°$, $\langle E_i \rangle$ (Ar) = 12.5 eV, and $T_s = 125$ K.

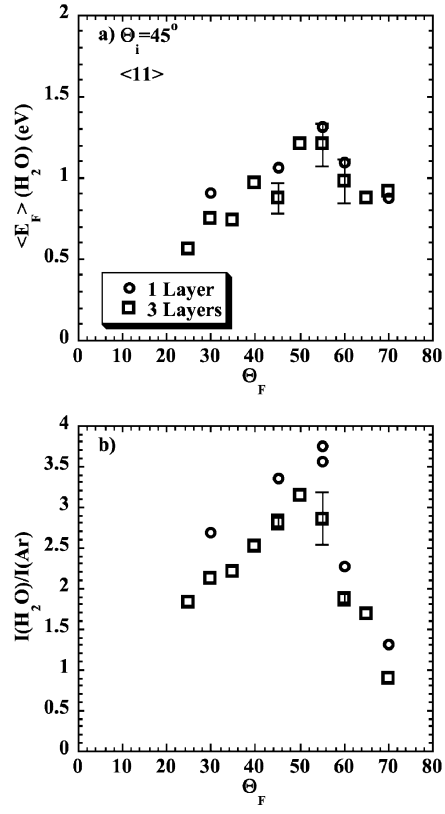

Figure 6. The average energy and integrated intensity for water molecules sputtered from one and three layers of H_2O as a function of Θ_f are plotted. Conditions are $\Theta_i = 45°$, <11> azimuth, an incident translational energy of 10.4 eV for the Ar, and $T_s = 125$ K.

distinct distributions. One distribution, due to the direct-inelastic (DI) channel, involves atoms that scatter directly from the surface at high energies with an intensity distribution that peaks superspecularly. The other distribution represents atoms that are

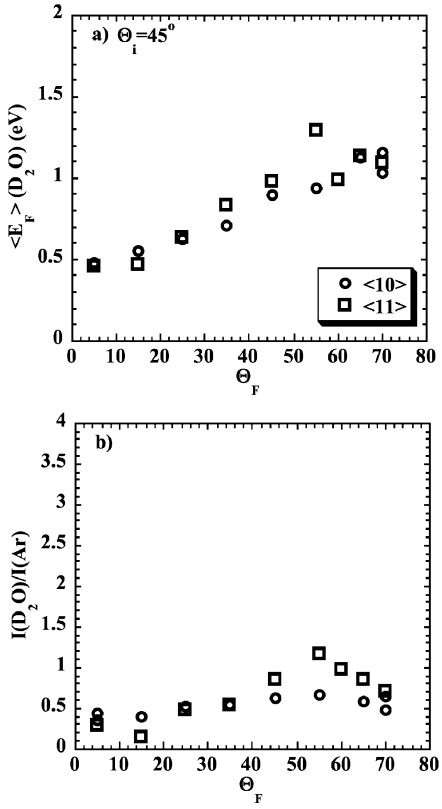

Figure 7. The average energy and integrated intensity for water molecules sputtered from eight layers of D_2O as a function of Θ_f for both the <10> and <11> azimuths are plotted. Conditions are $\Theta_i = 45°$, an incident translational energy of 12.1 eV for the Ar, and $T_s = 125$ K.

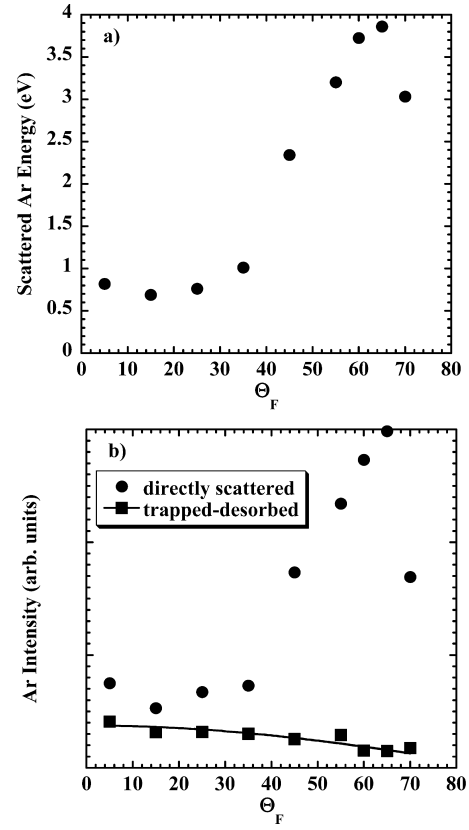

Figure 8. Shown are the average energy and integrated intensity for Ar scattering from eight layers of D_2O as a function of Θ_f along the <11> azimuth. Conditions are $\Theta_i = 45°$, an incident translational energy of 12.1 eV for the Ar, and $T_s = 125$ K. The energy plot shows the results for just the direct-inelastic component. The intensity plot shows the result for both the direct-inelastic and trapped-desorbed ($\langle E \rangle$ = 22 meV) components. The line through the trapped-desorbed data is $\cos(\Theta_f)$.

trapped on or near the surface long enough to thermalize and is referred to as the trapped-desorbed (TD) channel. These leave the surface with an average energy of 2 kT_s, where k is Boltzmann's constant, and have a $\cos(\Theta_f)$ angular intensity distribution. The results shown in Figure 8 are only for the in-plane scattering, and so under-represent the actual ratio of TD/DI. The direct-inelastic component will probably be concentrated at out-of-plane angles near the plane defined by the detector and the incident Ar beam, while the trapped-desorbed component will come off over the entire 2π steradians.

These results bring up the question of energy balance. A rough estimate for the energy needed to sputter a water molecule is 0.5 eV.[23,24] As shown in Figure 8, a large fraction of the incident Ar kinetic energy is certainly exchanged with the surface, but the sputtering yield, even for the monolayer, is very small, and the water that is sputtered only has at most a few times the minimum energy needed to escape. This demonstrates how well the ordered water overlayers can dissipate the energy of the collision. A possible analogy is the sputtering of alkanes from a Au(111) surface with hyperthermal Xe.[9] The sputtering yield is inversely proportional to the alkane length, and the low yields are attributed to the excitation of internal modes and loss to the substrate. For our experiments, the hydrogen-bonded network of the ice film acts as an effective sink, carrying away the energy imparted by the collision, resulting in a low sputtering yield.

Another consideration is the amount of surface damage. Even when the sputtering yield is low, it is still possible that many of the surface atoms are displaced.[25] This possibility was not examined directly, but the fact that there is a strong azimuthal dependence in the sputtering suggests that the accumulated damage is minimal. This could be due to the relatively warm surface (125 K), which allows for some surface annealing.

Conclusions

Ar atoms with a kinetic energy of 10−20 eV are able to sputter molecules from ordered overlayers of water grown on Rh(111). The sputtering is sensitive to the crystalline structure of the ice overlayers; the intensity and energy of the sputtered molecules are dependent on both the final polar and azimuthal angles. The similarity between the results for one and three layers of water strongly suggests that regardless of the precise details of the scattering mechanism leading to sputtering, it all occurs in the topmost layer. Sputtering yields are small, $\sim 10^{-3}$, and decrease with increasing film thickness. Most of the energy transferred during the collision is dissipated into the lattice. These results suggest that sputtering of surfaces with hyperthermal neutrals might be useful as a noncharging and nonchemically destructive adjunct to ion-induced sputtering and SIMS for compositional depth profiling and trace analysis. In this case intact, neutral molecules are ejected, and the molecules left on the surface have not been altered.

Acknowledgment. The authors acknowledge support from the Air Force Office of Scientific Research and the Army Research Office/DTRA, as well as the NSF-MRSEC at the University of Chicago, Grant NSF-DMR-0820054.

References and Notes

(1) Garrison, B. J.; Winograd, N. *Science* **1982**, *216*, 805.
(2) Yamamura, Y.; Takiguchi, T.; Kimura, H. *Nucl. Instrum. Methods Phys. Res., Sect. B* **1993**, *78*, 337.

(3) Gnaser, H. *Low-energy ion irradiation of solid surfaces*; Springer-Verlag: Berlin, 1999.

(4) *Sputtering by Particle Bombardment*; Behrisch, R., Eckstein, W., Eds.; Springer-Verlag: Berlin, 2007.

(5) Vu, B. Y.; Chen, Y. Y.; Wang, W. B.; Hsu, M. F.; Tsai, S. P.; Lin, W. C.; Lin, Y. C.; Jou, J. H.; Chu, C. W.; Shyue, J. *J. Anal. Chem.* **2008**, *80*, 3412.

(6) Bachman, B. J.; Vasile, M. J. *J. Vac. Sci. Technol., A* **1989**, *7*, 2709.

(7) Beckerle, J. D.; Johnson, A. D.; Ceyer, S. T. *J. Chem. Phys.* **1990**, *93*, 4047.

(8) Kulginov, D.; Persson, M.; Rettner, C. T. *J. Chem. Phys.* **1997**, *106*, 3370.

(9) Libuda, J.; Scoles, G. *J. Chem. Phys.* **2000**, *112*, 1522.

(10) Amirav, A.; Cardillo, M. J. *Surf. Sci.* **1988**, *198*, 192.

(11) Gibson, K. D.; Viste, M.; Sibener, S. J. *J. Chem. Phys.* **2000**, *112*, 9582.

(12) Fama, M.; Shi, J.; Baragiola, R. A. *Surf. Sci.* **2008**, *602*, 156.

(13) Brenner, D. W.; Garrison, B. J. *Phys. Rev. B: Condens. Matter* **1986**, *34*, 5782.

(14) Padowitz, D. F.; Sibener, S. J. *Surf. Sci.* **1991**, *254*, 125.

(15) Colonell, J. I.; Gibson, K. D.; Sibener, S. J. *J. Chem. Phys.* **1995**, *103*, 6677.

(16) Caledonia, G. E.; Krech, R. H.; Green, D. B. *AIAA J.* **1987**, *25*, 59.

(17) Zhang, J.; Garton, D. J.; Minton, T. K. *J. Chem. Phys.* **2002**, *117*, 6239.

(18) Proch, D.; Trickl, T. *Rev. Sci. Instrum.* **1988**, *60*, 713.

(19) Verdaguer, A.; Sacha, G. M.; Bluhm, H.; Salmeron, M. *Chem. Rev.* **2006**, *106*, 1478.

(20) Lilach, Y.; Romm, L.; Livneh, T.; Asscher, M. *J. Phys. Chem. B* **2001**, *105*, 2736.

(21) Romm, L.; Livneh, T.; Asscher, M. *J. Chem. Soc., Faraday Trans.* **1995**, *91*, 3655.

(22) Gibson, K. D.; Isa, N.; Sibener, S. J. *J. Chem. Phys.* **2003**, *119*, 13083.

(23) Petrenko, V. F.; Whitworth, R. W. *Physics of Ice*; Oxford University Press: Oxford, 1999.

(24) Smith, J. A.; Livingston, F. E.; George, S. M. *J. Phys. Chem. B* **2003**, *107*, 3871.

(25) Metiu, H.; DePristo, A. E. *J. Chem. Phys.* **1989**, *91*, 2735.

JP901874D